Freeze-drying as a Novel Concentrating Method for Wastewater Detection of SARS-CoV-2

Rui Dong[a], *Elizabeth Noriega Landa*[a], *Hugues Ouellet*[b], *Wen-Yee Lee*[a], Chuan Xiao[a]*

[a]*Department of Chemistry and Biochemistry, The University of Texas at El Paso, 500 W. University Ave, El Paso, TX 79902, USA*

[b]*Department of Biological Sciences, The University of Texas at El Paso, 500 W. University Ave, El Paso, TX 79902, USA*

Abstract

Detecting viral RNA from wastewater has emerged as a cost-effective approach for community-level surveillance during the recent SARS-CoV-2 pandemic. Although various concentrating methods have been developed, none are optimal for all key requirements for wastewater viral detection. Freeze-drying, a technique widely used for concentrating and preserving biological materials, remains underexplored for this purpose. This study compared the performance of freeze-drying and centrifugal ultrafiltration in terms of recovery efficiency, detection limit, and other key parameters. Early pandemic samples in this study, with extremely low viral concentrations, offered an ideal benchmark to assess their suitability for early-warning applications. Statistical analyses showed that freeze-drying achieved significantly higher recovery efficiency (20.2 ± 3.8% vs. 12.9 ± 2.0%), superior detection ratio (68.4% vs. 31.6%), and lower detection limit (0.06 vs. 0.35 copies/mL) compared to centrifugal ultrafiltration. To our knowledge, this is the first study to apply freeze-drying for wastewater-based viral detection. Despite its longer processing time, freeze-drying offers multiple advantages, including elimination of pretreatment steps, flexible storage, reduced RNA degradation under cryogenic conditions, minimal pathogen exposure, lower labor demands, and less human interference during processing. These features position freeze-drying as a novel alternative for wastewater-

based viral surveillance, particularly for developing early-warning systems in resource-limited settings.

Keywords: wastewater; viral RNA detection; SARS-CoV-2; concentrating; freeze-drying; centrifugal ultrafiltration.

---

* Corresponding Author. Tel.: +01-915-747-8657

Email Address: cxiao@utep.edu

1. Introduction

Coronavirus disease 2019 (COVID-19) is caused by the Severe Acute Respiratory Syndrome Coronavirus 2 (SARS-CoV-2), a single-stranded RNA virus. The World Health Organization has classified COVID-19 as a global pandemic. As of December 15, 2024, over 7 million deaths have been reported worldwide.[1,2] Timely detection and monitoring of the virus at the early stages of a pandemic are crucial to mitigate its spread, and wastewater surveillance has emerged as a recognized and effective approach. Notably, in March 2020, Medema et al. reported the first detection of SARS-CoV-2 RNA in wastewater in the Netherlands, preceding major outbreaks in various regions.[3-5] Quantifying SARS-CoV-2 viral RNA in sewage offers the possibility for developing an early alarm system, providing valuable insights into disease prevalence, and allowing public health authorities more time to intervene. Thus, a sensitive and cost-effective method will be desirable for such applications.

Nevertheless, assessing viral load within wastewater presents challenges due to the variable composition of sewage. Wastewater comprises both liquid and solid phases, each might contain viral signals.[3] Moreover, the composition of wastewater is influenced by numerous factors,

including local precipitation, drought conditions, temperature fluctuations, and water usage patterns.[4] Therefore, the concentration of viruses in wastewater can fluctuate widely. In addition, nucleases in the environment can potentially degrade nucleic acids, particularly RNA, representing another significant factor impacting detectable viral RNA concentration in wastewater.[5] Considering all these variables, detecting minute quantities of specific pathogens in the complex matrix of wastewater represents a substantial challenge, necessitating a proper sample concentrating method to maximize preservation of signal for subsequent detection.

To tackle these challenges, a concentrating method should be developed specifically to address the properties of wastewater. An effective method must efficiently collect viruses from both wastewater phases while protecting viral genomic materials from degradation. The method should avoid (1) pretreatments such as prefiltration that could result in loss of the viruses associated with solid particles;[6,7] (2) addition of chemicals that may inhibit downstream detection.[8–10] Additionally, especially for RNA viruses, the approach should minimize the degradation caused by ubiquitous environmental RNases.[11] Given the very low viral load during early and late pandemic stages (**Figure 1a**), the recovery rate and detection limit of concentrating method will be the most critical criterion. For resource-limited facilities such as those wastewater treatment plants, the concentrating method should be easy to establish without specialized personnel training. In addition, labor-intensive processes should be minimized in the protocol for long-term surveillance applications.[12]

The U.S. Centers for Disease Control and Prevention (CDC) has outlined five distinct methodologies for concentrating viral particles from wastewater.[13] While each of these methods employs different principles to address the challenges of low viral RNA content in wastewater,[6,14–19] none fully meet all the criteria for effectively concentrating and detecting

viruses. Achieving sensitive viral RNA detection in wastewater samples, especially during the onset of COVID-19 peaks with sporadic infections, necessitates the development of more strategic sample concentrating methods.

In contrast, freeze-drying, which is not listed by CDC, is a promising alternative concentrating method that is widely used to preserve various biological products.[20,21] Recently, it has been applied to concentrate wastewater samples to evaluate the deactivating effect of Fe^{3+} treatment on bacteria,[22] yet its potential for wastewater-based virus detection has not been explored. Freeze-drying effectively removes water from wastewater matrices by sublimation. This method uniquely retains viral entities from both the liquid and solid components of wastewater, which enhances detection sensitivity. Additionally, freeze-drying does not rely on reagent-dependent sample pre-treatment, thus preserving sample integrity from chemical interventions. The cryogenic environment during freeze-drying prevents the degradation of viral RNA, thereby improving the detection limit in the subsequent steps. Although it is time-consuming to process large-volume samples, freeze-drying offers operational convenience by minimizing human oversight after initial setup. In summary, freeze-drying represents a novel, sensitive, reliable, and less labor-intensive virus detection methodology, as it minimizes viral loss and optimizes the protection of viral RNA. Nevertheless, its effectiveness needs to be assessed by comparing to existing methods.

This study will be the first to apply freeze-drying to measure SARS-CoV-2 levels in wastewater. A comparative analysis was conducted between freeze-drying and widely used centrifugal ultrafiltration as concentrating methods for wastewater samples. Throughout the subsequent sections, “ultrafiltration” will be used in lieu of the more descriptive term "centrifugal ultrafiltration" to improve conciseness. Ultrafiltration was chosen for comparison because it is among the most widely used methods, having been employed in the first[23] and several early publications[24–26] on detecting SARS-CoV-2 in wastewater. Critical factors, including recovery efficiency and detection limits, were systematically compared and evaluated through RT-qPCR analyses across both concentrating methods.

The wastewater samples tested in this study held exceptional value as they were collected during the critical onset and waning phases of pandemic peaks. During these periods, viral concentrations were extremely low, highlighting the value of this comparison in selecting a better concentrating method for developing a wastewater-based early warning system. Before using these precious samples, thorough method testing and optimization have been carried out using DNA and RNA standards, as well as a similar but less pathogenic coronavirus. Although each invaluable sample was only processed by each concentrating method once due to volume limitation of sample collected in those pandemic periods, our optimal utilization strategy ensured reliable quantitative measurements while maximizing the extraction of meaningful epidemiological insights from these irreplaceable specimens. The resulting data are pivotal for developing a sensitive, precise, reproducible, and practical system to detect viruses in wastewater, ultimately enhancing community-level early warning and surveillance capabilities.

2. Material and Methods

2.1. Sample Collection and Pasteurization

Raw wastewater samples composited over 24 hours from the final effluent were collected on designated dates primarily during the early stages of the first COVID-19 pandemic peak in El Paso, Texas, USA, with additional samples collected during the low and steady tail of the peak (**Figure 1a, Supplementary Table S3**). Due to limited storage space in -80 °C freezers, only 500 mL of each sample was obtained. The wastewater samples were collected from four wastewater treatment plants (WWTPs) in El Paso, Texas, USA. These WWTPs are Haskell Street Wastewater Plant (HS), John T. Hickerson Water Reclamation Facility (JH), Fred Hervey Water Reclamation (FH), and Roberto R. Bustamante Wastewater Plant (BU). Locations of these WWTPs are shown in **Figure 1c**. Due to safety concerns during the early phase of the pandemic, before the person-to-person transmission pathway of the SARS-CoV-2 was elucidated (March 2020 to July 2020), a sample collecting protocol was developed and approved by the Institutional Biosafety Committee (IBC) of the University of Texas at El Paso (UTEP). Individuals collecting samples overcautiously wore double-layer disposable nitrile gloves, splash goggles, N95 or surgical masks, and disposable lab coats. Nevertheless, these overcautiously designed sample collection protocols can be used for future emerging viruses.

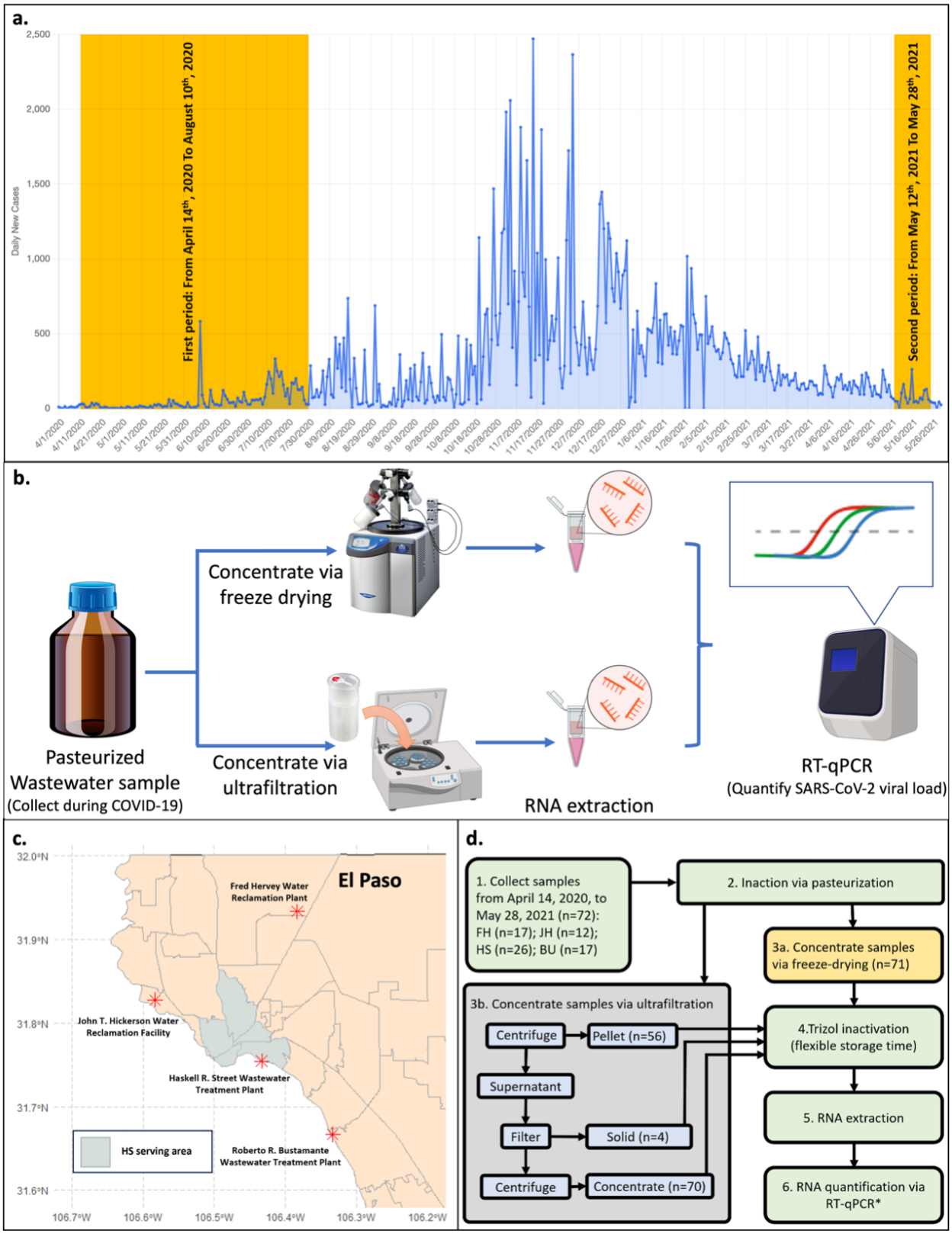
a.
Daily New Cases
2,500
2,000
1,500
1,000
500
0
First period: From April 14th, 2020 To August 10th, 2020
Second period: From May 12th, 2021 To May 28th, 2021
b.
Pasteurized Wastewater sample
(Collect during COVID-19)
Concentrate via freeze drying
Concentrate via ultrafiltration
RNA extraction
RT-qPCR
(Quantify SARS-CoV-2 viral load)
c.
El Paso
Fred Hervey Water Reclamation Plant
John T. Hickerson Water Reclamation Facility
Haskell R. Street Wastewater Treatment Plant
Roberto R. Bustamante Wastewater Treatment Plant
HS serving area
32.0°N
31.9°N
31.8°N
31.7°N
31.6°N
106.7°W
106.6°W
106.5°W
106.4°W
106.3°W
106.2°W
d.
1. Collect samples from April 14, 2020, to May 28, 2021 (n=72): FH (n=17); JH (n=12); HS (n=26); BU (n=17)
2. Inaction via pasteurization
3a. Concentrate samples via freeze-drying (n=71)
3b. Concentrate samples via ultrafiltration
Centrifuge
Pellet (n=56)
Supernatant
Filter
Solid (n=4)
Centrifuge
Concentrate (n=70)
4.Trizol inactivation (flexible storage time)
5. RNA extraction
6. RNA quantification via RT-qPCR*

126

127 **Figure 1.** Experimental design. **(a)** El Paso COVID-19 pandemic data. Daily new case numbers (blue) were plotted,
128 and the two sample collecting periods were shaded in orange. **(b)** Flow chart of comparing freeze-drying and
129 ultrafiltration as concentrating methods for wastewater virus detection. **(c)** El Paso area and water facility sites. Four
130 El Paso WWTPs were marked as red "*" and labeled on the map. El Paso area was colored pale orange. **(d)** Flow
131 chart of sample processing with sample numbers. Samples collected from four different WWTPs were inactivated
132 through pasteurization and then concentrated using two methods. FH, Fred Hervey Water Reclamation Plant; JH,
133 John T. Hickerson Water Reclamation Facility; HS, Haskell R. Street Wastewater Treatment Plant; BU, Roberto R.
134 Bustamante Wastewater Treatment Plant. The number (n) of samples processed at each step is indicated in
135 parentheses. Viral RNA of all the samples was extracted from concentrated samples and subjected to RT-qPCR for
136 quantification.

137 Samples were collected in the precleaned wide-mouth, leak-proof bottles (Fisherbrand™, Cat#
138 05719709), transported in double zip-lock bags within hard-plastic coolers to the BSL-2 lab, and
139 handled under standard biosafety and disinfection procedures. For early pandemic samples,
140 bottles were immediately frozen and stored at -80 °C following the overcautiously designed IBC
141 protocol in **Section 2.1.** Later, after CDC published its guideline to inactivate pathogens for
142 wastewater virus detection,[27] samples were pasteurized in a water bath at 65 °C for 90 min
143 before being stored at -80 °C. For those early sample without pasteurization, before processing,
144 they were thawed and pasteurized as recommended by the CDC guidelines.

145 **2.2. Sample Concentrating via Freeze-drying**

146 Although samples were pasteurized and thus considered to be biosafety level 1 (BSL-1) based
147 on the CDC guidelines,[12] a fully sealed freeze-drying set-up was overcautiously designed and
148 implemented using FreeZone 2.5 Liter -84 °C Benchtop Freeze Dryer (Labconco™, Cat#
149 710201000), this design is illustrated in **Figure 2**. The biosafety set-up incorporated multiple
150 safeguards: (1) The freeze dryer vacuum chamber contained PTFE coated coil, which is resistant

151 to erosive disinfectants that are used after each freeze-drying cycle; (2) Three layers of Filter
152 papers (Labconco™, Cat# 7544810) and aseptic valve (Labconco™, Cat# 7543900) were added
153 between the fast-freeze flask and manifold to prevent any potential accidental pathogen from
154 passing through; (3) A HEPA filter was added before the vacuum pump as the last filter to
155 capture any potential accidental pathogen leakage and spillage; (4) Wastewater samples were
156 placed inside plastic Erlenmeyer flasks which were wrapped with absorbent pads in 600 mL
157 Complete Fast-Freeze Flasks (Labconco™, Cat# 7540800). The absorbent pads were intended to
158 capture any accidental spill; and (5) The exhausting pipe of the vacuum pump was connected to
159 the chemical fume hood, to exhaust the odorous volatile organic compounds from the
160 wastewater. Even with these safety designs, as an extra precaution, all potentially contaminated
161 containers and the flow path before the HEPA filter were disinfected after each freeze-drying
162 run.

163 As shown in **Figure 1b and d**, prior to the freeze-drying procedure, 200 mL of each
164 pasteurized wastewater sample from **Section 2.1** was weighed and aliquoted into a 250 mL
165 plastic Erlenmeyer flask, wrapped with absorbent pads, placed into a zip-lock bag, and frozen
166 at -80 °C at least overnight. On the day of concentrating, the frozen samples in Erlenmeyer flasks
167 wrapped with absorbent pads were then placed in Fast-Freeze Flasks with plastic Erlenmeyer
168 flask caps loosened. Freeze-drying was conducted with temperature set to −86 °C and vacuum
169 to 0.040 mbar. After approximately three days of freeze-drying, sample masses were reduced to
170 about 3 g. Volume reduction factors were estimated by sample weight before and after freeze-
171 drying. The freeze-dried samples were dissolved in three volumes (v/w), approximately 9 mL, of
172 TRIzol™ LS reagent (Thermo Fisher Scientific, Cat # 10296-028). Samples were vortexed to
173 ensure thorough mixing before storing at –20 °C until viral RNA extraction. It has been proven

174 that TRIzol will deactivate all viral pathogens such as SARS-CoV-2 in the sample.[28] Therefore,
175 the following steps will be considered as BSL-1.
176

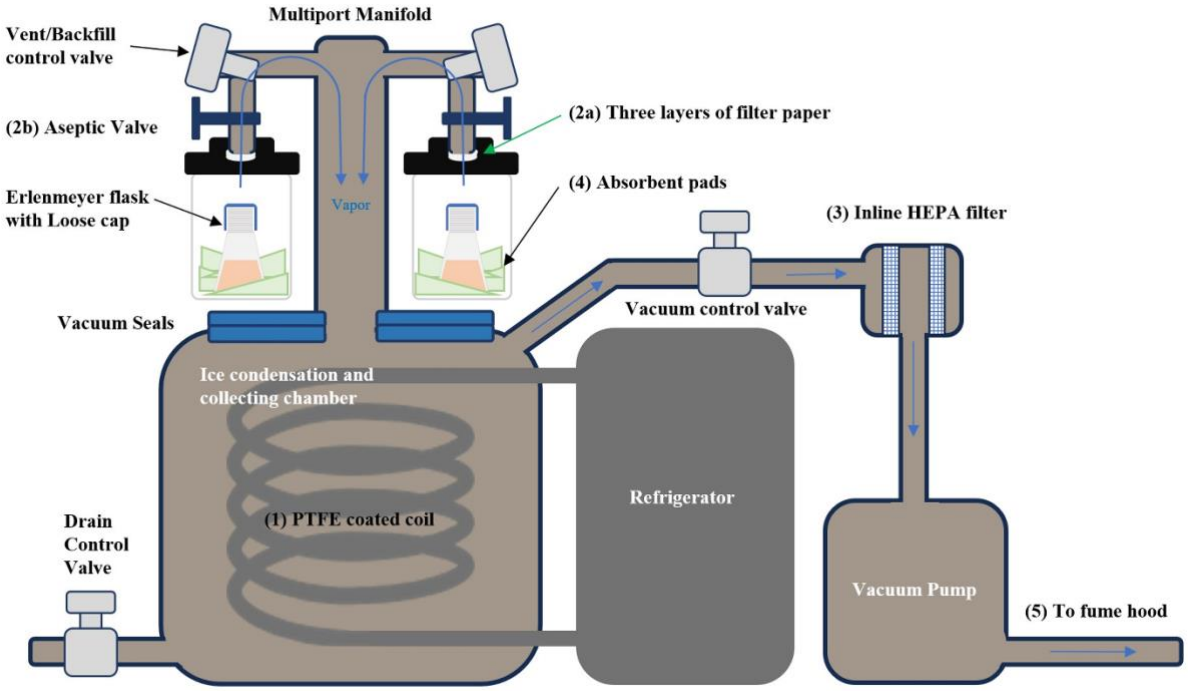

177

178 **Figure 2.** Schematic diagram of freeze-drying set-up. Key biosafety safeguard features are highlighted
179 and labeled with numbers within the diagram.

180 ## 2.3. Sample Concentrating via Ultrafiltration

181 In parallel to concentrating samples via freeze-drying as shown in **Figure 1b and d**, another
182 200 mL of pasteurized wastewater sample from **Section 2.1** was aliquoted into four 50 mL
183 conical tubes and loaded into swinging buckets (Thermo Fisher Scientific, Cat# 75003655) with
184 adaptors (Thermo Fisher Scientific, Cat# 75003683) for the TX-400 rotor (Thermo Fisher
185 Scientific, Cat# 75003181). The swinging buckets are sealed with ClickSeal Biocontainment
186 Lids (Thermo Fisher Scientific, Cat# 75003656) and wiped with disinfectant on the outside

before centrifuging at 3,000 × *g* for 15 min using Multifuge X1R Refrigerated Centrifuge (Thermo Fisher Scientific, Cat# 75004251). After centrifugation, the supernatant was filtered using a 0.22 µm PES bottle filter (Corning™, Cat# 431096) while the pellets were collected and weighed. Three volumes over the measured weight of TRIzol™ LS reagent were added to the pellet. All these procedures were carried out in a biosafety cabinet (BSC) to ensure safety. **Supplementary Figure S1** illustrates the filter system with multiple, overcautiously designed safeguards: (1) A trap bottle with disinfectant on the bottom was connected to the filter bottle to capture any potential accidental pathogen leakage and spillage; (2) An in-line 0.22 µm filter was added before the vacuum valve further to capture any potential accidental pathogen leakage and spillage.

Inside the BSC, the filtered supernatants from the previous step were aliquoted (approximately 70 mL) into Centricon Plus-70 with 10 kDa MW cut-off membrane (MilliporeSigma, Cat# UFC701008) and placed into disinfected swinging buckets (Thermo Fisher Scientific, Cat# 75003655, with seal cap Cat# 75003656). The buckets were completely sealed with ClickSeal Biocontainment Lids (Thermo Fisher Scientific, Cat# 75003656) and wiped with disinfectant on the outside before being taken out from BSC to be loaded onto TX-400 rotor (Thermo Fisher Scientific, Cat# 75003181). The samples were centrifuged at 3,500 × *g* for about 15 min using Multifuge X1R Refrigerated Centrifuge (Thermo Fisher Scientific, Cat# 75004251). After centrifugation, the swinging buckets were moved back into the BSC, and the passthrough liquid was disinfected and discarded. Following the same centrifugation protocol, the remaining filtered supernatants were added to Centricon Plus-70 units for the next round of concentrating via ultrafiltration.

209 After three to four rounds of centrifugation, the sample volume was reduced from 200 mL to
210 approximately 0.5 mL. Following the manufacturer's instructions, the filters were inverted and
211 centrifuged at 1,000 × *g* to collect the concentrates. The concentrated samples were subsequently
212 transferred to new tubes and mixed with three volumes, approximately 1.5 mL, of TRIzol™ LS
213 reagent. TRIzol treated samples were vortexed to ensure thorough mixing before being stored
214 at -20 °C until viral RNA extractions. Volume reduction factors for ultrafiltration were
215 determined by comparing the weights of the samples before and after concentrating. All the
216 filters and liquid transfer pipettes were soaked in ~1% bleach for at least 15 min before being
217 safely discarded.

218 **2.4. Viral RNA Extraction and Quantification**

219 SARS-CoV-2 RNA was extracted from the concentrated samples and purified using the
220 PureLink™ RNA Extraction Kit (Thermo Fisher Scientific, Cat# 12183018A). Prior to RNA
221 extraction, the frozen samples mixed with TRIzol were thawed at room temperature. For every
222 milliliter of sample mixed with TRIzol, 0.2 mL of Chloroform was added. The mixture was then
223 centrifuged at 12,000 × *g* at 4 °C for 30 min using ST16 Centrifuge (Thermo Fisher Scientific,
224 Cat# 75004381). Following centrifugation, the colorless upper aqueous phase, which contains
225 the RNA, was carefully extracted following the manufacturer's instructions. The bound RNA
226 was eluted from the spin cartridge in 30 µL of ribonuclease-free water and collected by
227 centrifugation. To maximize RNA recovery, second and third elutions were performed by adding
228 100 µL of ribonuclease-free water and centrifuging. The purified viral RNA was either
229 immediately analyzed by one-step RT–qPCR or stored at −20 °C to minimize degradation,
230 depending on thermocycler availability. RT–qPCR assays for RNA extracted from the same

231 sampling event but split and concentrated in parallel using the two methods, were always
232 performed in the same runs to ensure identical post-extraction processing.
233 SARS-CoV-2 RNA was quantified by one-step RT–qPCR using N1 and N2 primers sets
234 suggested by the CDC (**Table S1**).[29] Each sample was aliquoted in triplicate and analyzed using
235 the TaqPath™ 1-Step RT-qPCR (Thermo Fisher Scientific, Cat# A15299) in 20 μL reactions.
236 Triplicate water samples were added as the negative control. The qPCR reactions were run at 50
237 °C for 15 min and 95 °C for 2 min, followed by 45 cycles of 95 °C for 5 s and 55 °C for 30 s, per
238 the manufacturer's recommendations. The performance and efficiency of N1 and N2 primers in
239 the RT-qPCR assay were first evaluated by generating standard curves using 10-fold serial
240 dilution (1 to 10^5 copies per reaction) of templates: (1) a DNA plasmid containing complete
241 nucleocapsid gene from SARS-CoV-2 (IDT, Cat# 10006625), and (2) Twist synthetic SARS-
242 CoV-2 RNA (Twist Bioscience, Cat# MT0075s44). Standard curves and assay efficiency were
243 evaluated using Ct values from technical replicates as shown in **Figure 3** using similar methods
244 described in **Supplementary**
245 **Section 1.4**. To test template stability, standard curves were also generated after storage of
246 standards at -20 °C for up to four months. During the method development period with less than
247 four wastewater sample size with two concentration methods, a Magnetic Induction Cycler (Bio
248 Molecular System, Cat# 71-101, 48 reactions each in individual tubes). After the method was
249 optimized and standardized, the StepOnePlus™ Real-Time PCR System (Thermo Fisher
250 Scientific, Cat#4376600, 96 reactions in plates) was used with the same thermo cycling
251 conditions.
252 The original DNA and RNA stock had concentrations of 2.0×10^5 copies/μL and 1.0×10^6
253 copies/μL, respectively. Standard curves established from 10-fold dilutions of each DNA or

254 RNA stock with N1 or N2 assay were shown in **Figure 3**. The fresh DNA standard curve
255 generated using the N1 assay was used to quantify viral RNA in the concentrated wastewater
256 samples. Each RNA elution from extraction was aliquoted in triplicate and analyzed under
257 identical qPCR conditions as the standards. Each run included a no-template water negative
258 control. Viral concentrations were calculated as described in **Supplementary Section 1.3**. These
259 values represent the virus recovered by each concentrating method and therefore allow direct
260 comparison of their analytical sensitivity. Method-specific detection limits were determined by
261 the minimum detected concentration from all the wastewater samples using the same method
262 (**Supplementary Table S3** last row).

263 **2.5. Recovery Efficiency Calculations using Human Coronavirus OC43**

264 To compare the recovery efficiency of the two concentrating methods, human coronavirus
265 OC43 was chosen as the surrogate virus to be spiked into a wastewater sample. Both OC43 and
266 SARS-CoV-2 are beta-coronaviruses that cause respiratory infections in humans and are
267 transmitted via droplets and/or aerosols. However, unlike SARS-CoV-2, OC43 does not cause
268 severe disease in humans, making it an ideal surrogate for laboratory recovery tests without
269 biosafety concerns.

270 To estimate the amount of viruses to be spiked into wastewater for recovery efficiency
271 calculation, a standard curve of heat-inactivated OC43 virus was generated. The virus infectivity
272 of the original stock of heat-inactivated OC43 culture fluid (ZeptoMetrix, Cat# 0810024CFHI) is
273 defined by the median tissue culture infectious dose ($TCID_{50}$), the dilution of virus required to
274 infect 50% of the given cell monolayers.[30] An exact 100 μL aliquot of this inactivated OC43 at
275 5.0×10^{8} $TCID_{50}$/μL was used to prepare a 10-fold serial dilution with water. The concentration of
276 inactivated OC43 in each dilution was determined based on the dilution factor. These serially

277 diluted samples were then subjected to the same procedures aforementioned for TRIzol
278 treatment, RNA extraction, and RT-qPCR (triplets), but with different primer/probe sets for
279 OC43[31] (Sigma Custom DNA Oligos Cat# 41105327) (**Supplementary Table S1**). Following a
280 similar approach mentioned in **Section 2.4** for DNA and RNA standards, a standard curve was
281 established by plotting the RT-qPCR Ct value (*y*-axis) against the logarithm of heat-inactivated
282 OC43 concentration, expressed in the units of $TCID_{50}$.

283 To calculate the virus recovery efficiency of each concentrating method, an exact 20 μL aliquot
284 of Zeptometrix heat-inactivated OC43 with initial concentration of 5.0×10^{8} $TCID_{50}$/μL was
285 spiked into 400 mL pasteurized wastewater sample to reach a final concentration of 2.5×10^{4}
286 $TCID_{50}$/μL. To demonstrate that RT-qPCR cannot detect the virus without concentrating, 1 mL
287 of spiked sample was collected and treated with 3 mL of TRIzol™ LS reagent. The remaining
288 spiked sample was divided into two parts (approximately 200 mL each) and concentrated via
289 either freeze-drying or ultrafiltration, following the same procedure described in **Sections 2.2**
290 and **2.3** on sample concentrating. Viral RNA was then extracted and analyzed by RT-qPCR
291 (triplets) using the same procedure described previously for OC43 standard curve.

292 The Ct value from the RT-qPCR and the standard curve allowed the estimation of the
293 concentration of virus recovered by the two methods expressed in the unit of $TCID_{50}$/μL, which
294 can be used to calculate the total amount of virus recovered using the sample volumes
295 (**Supplementary Table S2**). Recovery efficiency was then calculated as the ratio of the
296 recovered virus amount to the amount initially spiked, with both values expressed in units of
297 $TCID_{50}$ (**Table 1**). The recovery efficiency estimations were performed in triplicate, allowing the
298 calculation of the mean and standard deviation for each method. A two-sample t-test, a

parametric test that assumes normal distribution of the data,[32] was conducted to determine whether there was a significant difference between the two methods.

2.6. COVID-19 Case Data and Statistical Analysis

Daily COVID-19 records from April 14, 2020, to May 28, 2021, in El Paso, TX, was collected from https://www.epstrong.org/results.php and https://elpasocovid19tracker.com/index.html (accessed 2025-11-18). Sampling dates with associated viral load calculations from all four wastewater plant sites are listed in **Supplementary Table S3**. The correlation between the total COVID-19 cases and SARS-CoV-2 viral load in wastewater was first evaluated for normality using the Shapiro-Wilk test.[33] Based on the results of the test, the Spearman's rank correlation was calculated between the total COVID-19 cases and SARS-CoV-2 viral load in wastewater, which can be denoted as rho "ρ".[34] This ρ, ranging from -1 to 1, provided a quantitative measure of the observed relationship between the two variables: daily COVID-19 case numbers and SARS-CoV-2 viral load in wastewater. A ρ close to zero means no correlation, while close to 1 and -1 indicate strong positive or negative correlation, respectively. All data processing and statistical analyses were conducted using R Studio.[35]

3. Results

3.1. Sample Collection

Our study underscores the importance of strict safety procedures when handling wastewater samples containing emerging pathogens, particularly in adhering to the stringent biosafety standards set by institutions such as the CDC and NIH. The designs of our wastewater sample collection and processing protocols reflect a strong commitment to these high safety standards. A

320 multilayer safety setup was implemented during sample collection and pasteurization, including
321 the use of disposable protective gear, rigorous disinfection protocols, and an approved safety
322 protocol developed early in the SARS-CoV-2 pandemic. This proactive approach to biosafety
323 was crucial during uncertain times. Combining sample collection with immediate pasteurization,
324 a swift transition to BSL-1 became possible, offering a versatile solution for handling unknown
325 emerging pathogens. This approach is particularly beneficial for laboratories with limited
326 resources, such as those affiliated with wastewater treatment plants.

327 A total of 83 wastewater samples were collected from four wastewater treatment plants
328 (WWTPs) in El Paso, Texas (**Figure 1d**), USA, from April 14, 2020, to May 28, 2021. Given
329 that our wastewater samples were collected from the onset and waning phases of pandemic
330 peaks, the anticipated viral concentration was extremely low, making these samples especially
331 valuable for detection and quantification comparison. However, our storage capacity was
332 severely limited, restricting both the volume of wastewater that could be retained and the total
333 number of samples processed. These constraints meant that only 500 mL of wastewater could be
334 collected for each sampling event, and each sample was split into two 200 mL portions, which
335 were analyzed in parallel by the two concentrating methods once. However, triplicate RT-qPCR
336 analyses were performed on RNA extracted from the concentrated samples, maximizing the
337 usage of each collection and allowing us to obtain reliable quantitative measurements despite
338 challenging sample availability. Our study design reflects careful stewardship and maximization
339 of these precious materials, demonstrating a commitment to extracting the most meaningful data
340 possible within logistical and epidemiological limitations. Corresponding local daily case
341 numbers were shown in **Figure 1a**. However, some samples from certain WWTPs were
342 unavailable due to technical and personnel challenges encountered during the pandemic. During

343 the small peaks from April 2020 to August 2020, 60 samples were collected and stored in
344 a -80 °C freezer using sample collection protocol at UTEP before the analytic protocol was fully
345 developed and approved by IBC. Due to the limited lab accessibility during the pandemic,
346 human resource constraints, and the restricted storage space in -80 °C freezers, sample collection
347 was paused between August 2020 and April 2021. Once the samples were processed using the
348 fully developed and approved protocol and storage space was freed up in -80 °C freezers, sample
349 collection was resumed in May 2021. The collection frequency during the second period was
350 more sporadic, depending on the processing speed of stored samples. For the second period, a
351 total of 12 samples were collected. Following pasteurization to inactivate wastewater pathogens,
352 71 samples were concentrated using freeze-drying and 70 using ultrafiltration, respectively.
353 Additionally, 56 pellets were collected from 70 ultrafiltration samples (**Figure 1d**).
354 Unfortunately, RT-qPCR data for 11 samples were lost due to an unexpected crash of the
355 computer that controls the StepOnePlus™ Real-Time PCR System. At the end, data from a total
356 of 72 samples were obtained (**Figure 1d**, **Table S3**).

357 **3.2. RT-qPCR Primer Selection and Template Stabilities**

358 Standard curve analysis in **Figure 3** shows that across all points of RNA and DNA standards,
359 the N1 primer consistently exhibited higher R^2 values and lower Ct values than the N2 primer,
360 indicating a stronger linear correlation between the measured and expected quantities.
361 Additionally, the fitted lines of N1 for both RNA and DNA are lower than those of N2, reflecting
362 overall lower Ct values for the N1 primer. These higher R^2 values and lower overall Ct values
363 highlight the superior quantification accuracy and reliability of the N1 primer, making it the
364 preferred choice. However, the impact of standards degradation over time cannot be overlooked,
365 as evidenced by the progressive increase in the heights (Ct values) of fitting lines observed for

366 both RNA and DNA standards. Obviously, RNA exhibited more significant degradation than
367 DNA underscoring its higher susceptibility to degradation. The crossing observed in the RNA
368 and DNA standard curves using N2 primers after storage in -20 °C for 4 months (**Figure 3b** and
369 **Figure 3d)** suggests that the N2 primer region may be more susceptible to degradation, resulting
370 in deviations from the expected slope (approximately -3.3 to -3.4)[36] of the standard curve.
371 Consequently, while the N1 primer is the optimal choice for fresh samples due to its stronger
372 linear correlation, DNA standards are more suitable for long-term studies or situations requiring
373 extended sample storage, owing to its greater stability. Therefore, for the subsequent analyses,
374 we used DNA standards and N1 assay to estimate the total number of detected viruses.
375 Based on the observed degradation of RNA standard, specific precautions must be followed to
376 mitigate RNA degradation in concentrated wastewater and preserve its integrity for potential
377 future analyses. Immediate sample processing post-collection is ideal for maximizing RNA
378 extraction yield and maintaining its integrity. However, logistical constraints often necessitate
379 sample storage, for which TRIzol or similar denaturing reagents are highly recommended.
380 TRIzol effectively inhibits RNase activity, thereby preventing RNA degradation.[37] Concentrated
381 samples in TRIzol demonstrate superior stability for long-term storage, particularly when stored
382 at -80 °C freezer.[38] Thus, maintaining samples in TRIzol without RNA extraction until imminent
383 RT-qPCR analysis is considered the optimal storage strategy. Moreover, minimizing freeze-thaw
384 cycles of samples, regardless of the storage method, is critical to prevent RNA degradation.
385 RNases are prevalent and can regain enzymatic activity after removing denaturing conditions.[39]
386 Consequently, after RNA is extracted from the TRIzol storage solution, downstream procedures
387 should be performed promptly to minimize RNA degradation and ensure the reliability and
388 accuracy of the subsequent RT-qPCR analyses.

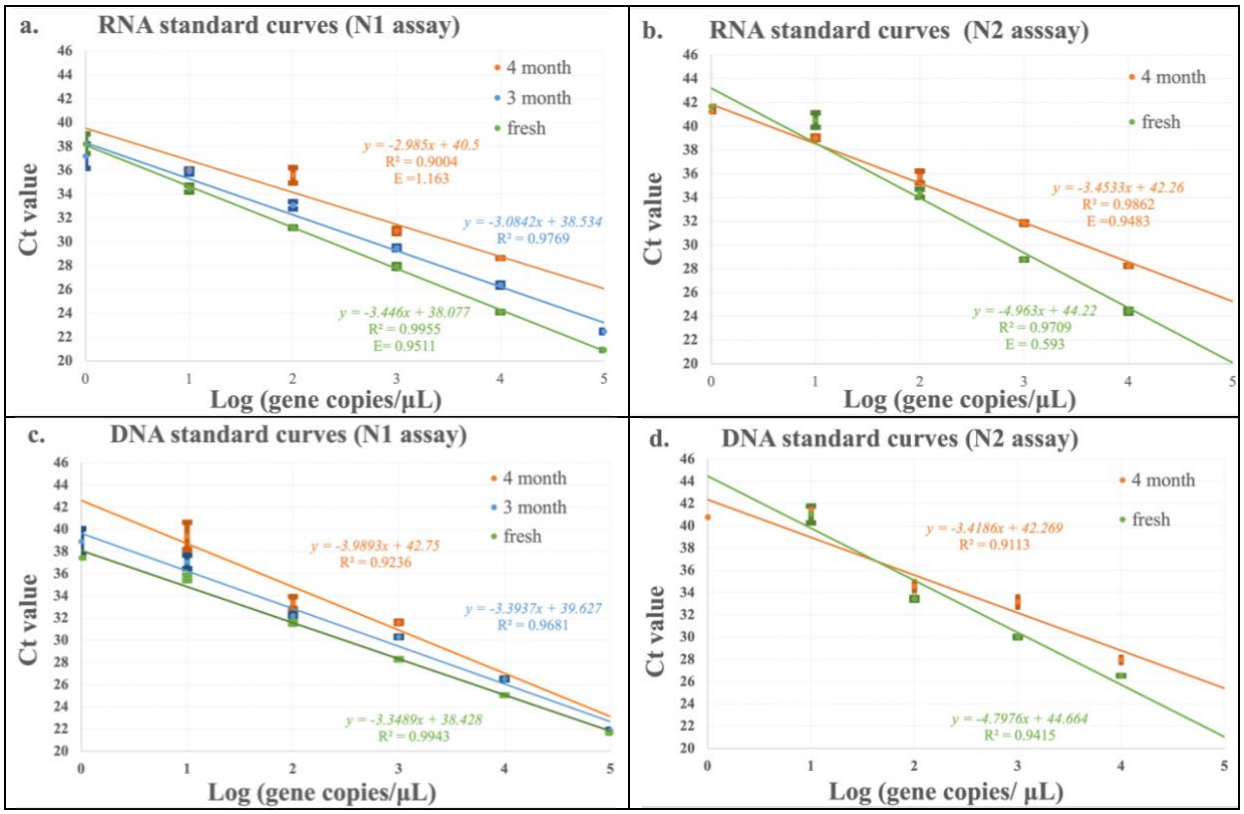

Figure 3. RNA and DNA standard curves. Panels a and b display the fitted lines of qPCR Ct mean values (*y*-axis) with error bars denoting ± SD, plotted against logarithm of gene copies (*x*-axis) of serially diluted RNA standards, using the N1 and N2 primers, respectively. Panels c and d present similar fitted lines for DNA standards. As the legend indicates, the different line colors represent standard curves generated from fresh samples or samples stored at -20 °C for 3 or 4 months. The fitted equations and corresponding R^2 values are shown in the same colors as their respective lines.

3.3. Comparison of Recovery Efficiency Between Two Concentrating Methods

Recovery efficiency for the two concentrating methods was compared using a surrogate virus: human OC43. Based on the standard curve using heat-inactivated OC43 virus (approximately 1.0 × 10^9 $TCID_{50}$) was spiked into 400 mL of wastewater. This sample was divided into two equal volumes and concentrated using either freeze-drying or ultrafiltration methods. A control sample without concentrating had an undetermined Ct value, indicating that RT-qPCR could not detect

401 the OC43 signal prior to concentrating. Recovery rates were calculated from the Ct values of the
402 first RNA extraction elution and were 20.2% for the freeze-drying method and 12.9% for the
403 ultrafiltration method. The higher recovery efficiency from the freeze-drying method was found
404 to be significant ($p = 0.04$) over that of the ultrafiltration method (**Table 1**).
405
406 **Table 1.** Recovery rate of freeze-drying and ultrafiltration

Method	Recovered virus ($TCID_{50}$)	Recovery rate (± SD）	p-value[1]
Freeze drying	1.08×10^9	20.2% (± 3.76)	0.04
Ultrafiltration	6.90×10^8	12.9% (± 1.95)	

407 [1] p-value obtained from two-sample t-test between the recovery rates from the methods of freeze-
408 drying and ultrafiltration.
409
410 Notably, the second elution from the freeze-dried sample exhibited a lower Ct value than the
411 first elution (**Supplementary Table S3**). This phenomenon was also observed in other
412 wastewater samples concentrated by freeze-drying during SARS-CoV-2 detection but not in the
413 sample concentrated via ultrafiltration or RNA extracted from heat-inactivated OC43 serial
414 dilution when establishing the standard curve. Since the freeze-drying process concentrates all
415 small molecules, it is possible that inhibitory substances affecting RT-qPCR may also be
416 enriched. When combining the recovery rates from both the first and second elutions, the overall
417 recovery rates remained at 20.2% for freeze-drying and 12.9% for ultrafiltration, demonstrating
418 the potential advantage of the freeze-drying approach.

419 **3.4. Comparison of Early Detection of Two Concentrating Methods**

420 To evaluate the detection sensitivities of the freeze-drying and ultrafiltration methods,
421 wastewater viral load data from the early stages of the COVID-19 pandemic (April 2020 to May
422 2020) were analyzed. A total of 38 samples were collected from various wastewater treatment
423 plants in El Paso, Texas, USA. The freeze-drying method identified 26 positive samples (68.4%)
424 (**Table 2**). As previously discussed, the freeze-drying method yielded lower Ct values (indicating
425 more sensitive detection) in the second elutions. When the second elution was included, the
426 detection ratio increased to 28 positive samples (73.7%). In contrast, the ultrafiltration detected
427 only 12 positive samples (31.6%), which increased slightly to 13 positive samples (34.2%) when
428 including the second elution (**Table 2**). The higher detection ratio observed with the freeze-
429 drying method highlights its superior ability to concentrate viral material compared to
430 ultrafiltration. This is particularly important given that our samples were collected during the
431 early stages of the pandemic, when viral loads in wastewater were extremely low (**Figure 1a**).
432 The higher detection ratio observed with the freeze-drying method suggests it is a more effective
433 approach for establishing an early warning system for the surveillance of emerging viruses.

434 The superior detection sensitivity of the freeze-drying method was further supported by the
435 lower average Ct values obtained during RT-qPCR analyses. Across all four wastewater
436 treatment plants, the freeze-drying method consistently exhibited lower Ct values compared to
437 ultrafiltration (**Table 2**), equivalent to a higher amount of viral RNA in the concentrated samples
438 (**Supplementary Table S3**). Furthermore, a Wilcoxon rank-sum test, a nonparametric test that
439 compares two independent groups without assumption of normal distribution,[40] was conducted to
440 compare virus copies in the original wastewater samples across all four facilities. As described in
441 **Section 2.4**, the total virus copies were estimated using the DNA standard curve and the Ct

442 values. For both freeze-dry and ultrafiltration methods, both first and second elutions were
443 combined to calculate the total RNA copies in the original wastewater samples. Where a method
444 or elution did not detect the virus, it was recorded as zero copies. A total of 72 data pairs from all
445 collected data listed in **Table S2** showed that there was a significant ($p = 5.70 \times 10^{-6}$) difference
446 between the detected virus concentration from the freeze-drying and the ultrafiltration methods.
447 As described in **Section 2.4**, method-specific detection limits of copies/mL can be determined
448 using the highest Ct value for each method and the standard curves. The freeze-drying method
449 demonstrated a lower limit of detection (0.06 copies/mL) compared to ultrafiltration (0.35
450 copies/mL) (**Supplementary Table S3** last row).

451

452 **Table 2.** Positive rate and Ct value range for samples collected from four WWTPs between April
453 2020 to May 2020

Site	Sample Number	Positive numbers		Positive Rate %		Range of Ct Value	
		Freeze-drying	Ultrafiltration	Freeze-drying	Ultrafiltration	Freeze-drying	Ultrafiltration
HS	18	12 (14)	5 (6)	66.7 (77.8)	27.8 (33.3)	31 (32) – 42 (42)	33 (33) – 38 (38)
JH	1	1 (1)	1 (1)	100.0 (100.0)	100.0 (100.0)	33 (33) – 33 (35)	35 (35) – 36 (36)
FH	8	6 (6)	5 (5)	75.0 (75.0)	62.5 (62.5)	32 (32) – 39 (39)	32 (32) – 41 (41)
BU	11	7 (7)	1 (1)	63.6 (63.6)	9.1 (9.1)	33 (33) – 37(37)	33 (33) – 34 (34)
Total	38	26 (28)	12 (13)	68.4 (73.7)	31.6 (34.2)		

454 * Numbers in the parentheses are values obtained from the second elution

455

3.5. Correlation Between Wastewater Viral Load and COVID-19 Case Numbers

The relationship between wastewater viral load and community COVID-19 cases is a key consideration in evaluating the utility of wastewater surveillance. The correlation between the measured viral load in wastewater and the reported COVID-19 cases in El Paso, TX, USA, was investigated. Available viral load data from Haskell Street Wastewater Plant and the corresponding daily COVID-19 case counts on the wastewater sample collection dates were collected. The areas from where the case numbers were collected cover HS serving regions, including zip codes 79901, 79902, 79903, 79905, and 79930 (**Figure 1c**).

Normalization of viral load data to accurately account for differences in human contribution to wastewater is widely considered essential in wastewater surveillance. Some studies use creatinine as a normalization biomarker to improve the correlation between wastewater viral loads and COVID-19 case trends.[41,42] Attempts following these studies were carried out via creatinine measurement using a commercial colorimetric kit (**Supplementary Section 1.5**). However, the concentrations of creatinine measured in the collected samples (**Supplementary Section 1.5**) were consistently below the kit's sensitivity limit, preventing reliable normalization, similar to the other report.[41] Given these analytical constraints and the primary goal of comparing two concentrating methods, the correlation analysis in this study was conducted on unnormalized data. Therefore, the correlation results presented here are meant to provide supplemental insight into the relationship between wastewater viral concentrations and community COVID-19 case counts, rather than to serve as definitive epidemiological findings.

Shapiro-Wilk tests showed $p = 5.6 \times 10^{-6}$, 8.4×10^{-5}, and 1.2×10^{-5}, for total RNA copies detected by freeze-drying, those detected by ultrafiltration, and community COVID-19 case numbers, respectively. Thus, it was concluded that these data were not normally distributed.

Given the small sample size, a non-parametric test was chosen instead of a parametric test.[33,43] The Spearman rank correlation test[34] was applied to evaluate the association between the total viral load and the number of reported daily cases on each date across the studied areas. Due to the unavailability of active case numbers during the early stages of the pandemic (April 2020 to May 2020), the analysis was conducted using daily case numbers. During this period, the difference among active, daily, and cumulative cases was likely minimal. Additionally, prior studies have indicated that recovered patients may continue shedding the virus.[44,45] During the early period, the analysis revealed a positive correlation of 0.45 between the freeze-dried viral load and the daily case numbers. This correlation was statistically significant ($p=0.048$). Similarly, for the ultrafiltration method, using data from the same period, the analysis showed a moderate positive correlation of 0.24 between the viral load and the cumulative COVID-19 case numbers, which was not statistically significant ($p=0.305$). Our results are consistent with various correlations found in published studies, some demonstrated a positive correlation[23,46] while other studies have reported weaker or inconsistent correlations[47]. These variations are potentially due to factors such as differences in viral shedding patterns and in testing rates, as well as the influence of local conditions on viral transport and persistence in wastewater systems.[48] It is important to note that the correlation observed in this study is mostly based on minimal data from the early stages of the pandemic and lacks reliable normalization of human contribution to wastewater.

4. Discussion

The two concentrating methods, ultrafiltration and freeze-drying, exhibited distinct disadvantages in performance and methodology in this study. Ultrafiltration requires multiple

502 pretreatment steps, such as centrifugation and filtration, to remove larger solids. However, this
503 process can inadvertently lead to the loss of viral signals that are associated with sewage
504 sludge.[49,50] This was confirmed by the viral signal detected in the pellet from the prefiltration
505 step (**Supplementary Table S2**). The same observation was also reported in literature, where
506 viral detection rate is commonly decreased when solids are excluded from wastewater samples.[51]
507 On the other hand, the major disadvantage of freeze-drying is its long processing time, where
508 one overnight deep-freezing process and around three days are needed to concentrate a 200 mL
509 sample to a target volume of approximately 3 mL.

510 Although freeze-drying has a longer processing time, it demonstrated a superior recovery rate
511 and lower detection limit compared to ultrafiltration in this study. This makes freeze-drying
512 particularly advantageous for early detection of viral pathogens during the onset or waning
513 phases of a pandemic (**Figure 1a**) when viral loads in wastewater are extremely low. This
514 superior performance can be attributed to several factors. Unlike ultrafiltration, freeze-drying
515 eliminates the need for prefiltration by retaining all wastewater components, including solids,
516 thereby maximizing viral capture, particularly for viruses associated with sewage sludge that
517 would otherwise be lost in the pretreatment of centrifugation and filtration. The process of
518 freeze-drying involves fewer liquid handling steps, reducing the opportunity for sample loss and
519 contamination. In addition, the immediate freezing of samples at −80 °C after pasteurization and
520 maintaining the sample throughout concentrating at ultra-low temperatures reduces the
521 degradation of viral RNA and preserves its integrity prior to downstream processing. This is
522 most important for RNA viruses due to the ubiquitous existence of RNase in the environment.
523 Additionally, the improved retention and processing fidelity achieved by freeze-drying is

524 reflected in stronger correlations between wastewater viral loads and community case data,
525 supporting its reliability for tracking disease prevalence through wastewater surveillance.
526 From the operational aspects, ultrafiltration uses expensive filters and involves multiple
527 centrifugation and liquid handling steps. These steps prolong operator exposure to wastewater
528 and increase pathogen transmission risks. Consequently, when working with unknown emerging
529 pathogens, ultrafiltration requires rigorous personal protective equipment (PPE) and extensive
530 decontamination procedures, resulting in labor-intensive workflows and limiting the throughput
531 to approximately eight samples per day. In contrast, the freeze-drying method uses only
532 inexpensive sample bottles and minimizes operator exposure, requiring brief handling for cap
533 loosening and flask mounting (**Figure 2**) during the initial setup. Decontamination was only
534 needed at process completion. Although the freeze-drying method does require three days to
535 concentrate eight samples, it demands minimal labor, reduces exposure to wastewater, and
536 minimizes human-factor variability during the whole process period (**Section 2.3**).
537 In summary, using invaluable samples collected mainly during the onset of the COVID-19
538 pandemic, this study conclusively demonstrated the superior performance of freeze-drying
539 method over the widely used ultrafiltration technique for concentrating wastewater samples for
540 viral detection. Freeze-drying's higher recovery rates, detection ratios, and sensitivity for viral
541 RNA in wastewater are crucial during periods when viral loads are low, such as the early phase
542 of a pandemic. Freeze-drying's operational benefits include increased storage flexibility, reduced
543 labor intensity, minimized exposure risks are particularly suitable for settings with limited
544 technical expertise. All these advantages of freeze-drying position it as a novel sensitive, precise,
545 reproducible, and practical method for early warning and surveillance applications against
546 emerging pathogens in the community.

ACKNOWLEDGMENT

During the preparation of this work, the author(s) utilized ChatGPT to only enhance readability and improve language. Following its use, the authors carefully reviewed and edited the content as necessary and took full responsibility for the final version of the publication. The authors would like to acknowledge Teresa T. Alcala and El Paso Water Laboratory personnel: Hugo Ruiz at John T. Hickerson Water Reclamation Facility, Martin L. Ortiz at Roberto Bustamante Wastewater Plant, Rick Dominguez at Haskell Street Wastewater Plant, Roberto Hernandez at Fred Hervey Water Reclamation, for their assistance during wastewater sample collection especially during the COVID-19 pandemic period. This work received funding from the College of Science, University of Texas at El Paso. The work has used instruments in the Border Biomedical Research Center (BBRC) that is supported by the National Institutes on Minority Health and Health Disparities (NIMHD) of the National Institutes of Health (NIH) under award number U54MD007592. Special thanks go to BBRC personnel Georgialina Rodriguez and Ana P. Betancourt who helped us use the instruments. RD and CX also received support from the National Institute of General Medical Sciences (NIGMS) of NIH under award number R01GM129525 and from the Welch Foundation under Grant Number AH-2126-20220331. WYL received support from NIGMS of NIH under the award number SC1CA245675. The content is solely the responsibility of the authors and does not necessarily represent the official views of the funding agencies.

REFERENCES

(1) World Health Organization. *Coronavirus Disease (COVID-19): Situation Report, 158*; World Health Organization, 2020. https://apps.who.int/iris/handle/10665/332858 (accessed 2022-02-14).

(2) CDC. *COVID Data Tracker*. Centers for Disease Control and Prevention. https://covid.cdc.gov/covid-data-tracker (accessed 2022-02-14).

(3) Roldan-Hernandez, L.; Boehm, A. B. Adsorption of Respiratory Syncytial Virus, Rhinovirus, SARS-CoV-2, and F+ Bacteriophage MS2 RNA onto Wastewater Solids from Raw Wastewater. *Environ. Sci. Technol.* **2023**, *57* (36), 13346–13355. https://doi.org/10.1021/acs.est.3c03376.

(4) Hughes, J.; Cowper-Heays, K.; Olesson, E.; Bell, R.; Stroombergen, A. Impacts and Implications of Climate Change on Wastewater Systems: A New Zealand Perspective. *Clim. Risk Manag.* **2021**, *31*, 100262. https://doi.org/10.1016/j.crm.2020.100262.

(5) Farkas, K.; Hillary, L. S.; Malham, S. K.; McDonald, J. E.; Jones, D. L. Wastewater and Public Health: The Potential of Wastewater Surveillance for Monitoring COVID-19. *Curr. Opin. Environ. Sci. Health* **2020**, *17*, 14–20. https://doi.org/10.1016/j.coesh.2020.06.001.

(6) Zheng, X.; Deng, Y.; Xu, X.; Li, S.; Zhang, Y.; Ding, J.; On, H. Y.; Lai, J. C. C.; In Yau, C.; Chin, A. W. H.; Poon, L. L. M.; Tun, H. M.; Zhang, T. Comparison of Virus Concentration Methods and RNA Extraction Methods for SARS-CoV-2 Wastewater Surveillance. *Sci. Total Environ.* **2022**, *824*, 153687. https://doi.org/10.1016/j.scitotenv.2022.153687.

(7) Banadaki, M. D.; Torabi, S.; Rockward, A.; Strike, W. D.; Noble, A.; Keck, J. W.; Berry, S. M. Simple SARS-CoV-2 Concentration Methods for Wastewater Surveillance in Low Resource Settings. *Sci. Total Environ.* **2024**, *912*, 168782. https://doi.org/10.1016/j.scitotenv.2023.168782.

(8) Zafeiriadou, A.; Nano, K.; Thomaidis, N. S.; Markou, A. Evaluation of PCR-Enhancing Approaches to Reduce Inhibition in Wastewater Samples and Enhance Viral Load Measurements. *Sci. Total Environ.* **2024**, *955*, 176768. https://doi.org/10.1016/j.scitotenv.2024.176768.

(9) Huge, B. J.; North, D.; Mousseau, C. B.; Bibby, K.; Dovichi, N. J.; Champion, M. M. Comparison of RT-dPCR and RT-qPCR and the Effects of Freeze–Thaw Cycle and Glycine Release Buffer for Wastewater SARS-CoV-2 Analysis. *Sci. Rep.* **2022**, *12* (1), 20641. https://doi.org/10.1038/s41598-022-25187-1.

(10) Ahmed, W.; Simpson, S. L.; Bertsch, P. M.; Bibby, K.; Bivins, A.; Blackall, L. L.; Bofill-Mas, S.; Bosch, A.; Brandão, J.; Choi, P. M.; Ciesielski, M.; Donner, E.; D'Souza, N.; Farnleitner, A. H.; Gerrity, D.; Gonzalez, R.; Griffith, J. F.; Gyawali, P.; Haas, C. N.; Hamilton, K. A.; Hapuarachchi, H. C.; Harwood, V. J.; Haque, R.; Jackson, G.; Khan, S. J.; Khan, W.; Kitajima, M.; Korajkic, A.; La Rosa, G.; Layton, B. A.; Lipp, E.; McLellan, S. L.; McMinn, B.; Medema, G.; Metcalfe, S.; Meijer, W. G.; Mueller, J. F.; Murphy, H.; Naughton, C. C.; Noble, R. T.; Payyappat, S.; Petterson, S.; Pitkänen, T.; Rajal, V. B.; Reyneke, B.; Roman, F. A.; Rose, J. B.; Rusiñol, M.; Sadowsky, M. J.; Sala-Comorera, L.; Setoh, Y. X.; Sherchan, S. P.; Sirikanchana, K.; Smith, W.; Steele, J. A.; Sabburg, R.; Symonds, E. M.; Thai, P.; Thomas, K. V.; Tynan, J.; Toze, S.; Thompson, J.; Whiteley, A. S.; Wong, J. C. C.; Sano, D.; Wuertz, S.; Xagoraraki, I.; Zhang, Q.; Zimmer-Faust, A. G.; Shanks, O. C. Minimizing Errors in RT-PCR Detection and Quantification of SARS-CoV-2

RNA for Wastewater Surveillance. *Sci. Total Environ.* **2022**, *805*, 149877. https://doi.org/10.1016/j.scitotenv.2021.149877.

(11) Sanchez-Quete, F.; Chiang, L.; Caldera Sequeira, F.; Goitom, E.; Tsitouras, A.; Maere, T.; Vanrolleghem, P. A.; Dorner, S.; Frigon, D.; Loeb, S. K. Suspended Solids and Optimal RNase Inhibitors Impact the Partitioning and Decay of SARS-CoV-2 in Wastewater. *ACS EST Water* **2024**, *4* (12), 5980–5988. https://doi.org/10.1021/acsestwater.4c01074.

(12) Juel, M. A. I.; Stark, N.; Nicolosi, B.; Lontai, J.; Lambirth, K.; Schlueter, J.; Gibas, C.; Munir, M. Performance Evaluation of Virus Concentration Methods for Implementing SARS-CoV-2 Wastewater Based Epidemiology Emphasizing Quick Data Turnaround. *Sci. Total Environ.* **2021**, *801*, 149656. https://doi.org/10.1016/j.scitotenv.2021.149656.

(13) Parkins, M. D.; Lee, B. E.; Acosta, N.; Bautista, M.; Hubert, C. R. J.; Hrudey, S. E.; Frankowski, K.; Pang, X.-L. Wastewater-Based Surveillance as a Tool for Public Health Action: SARS-CoV-2 and Beyond. *Clin. Microbiol. Rev. 37* (1), e00103-22. https://doi.org/10.1128/cmr.00103-22.

(14) Lu, D.; Huang, Z.; Luo, J.; Zhang, X.; Sha, S. Primary Concentration – The Critical Step in Implementing the Wastewater Based Epidemiology for the COVID-19 Pandemic: A Mini-Review. *Sci. Total Environ.* **2020**, *747*, 141245. https://doi.org/10.1016/j.scitotenv.2020.141245.

(15) Farkas, K.; Pellett, C.; Alex-Sanders, N.; Bridgman, M. T. P.; Corbishley, A.; Grimsley, J. M. S.; Kasprzyk-Hordern, B.; Kevill, J. L.; Pântea, I.; Richardson-O'Neill, I. S.; Lambert-Slosarska, K.; Woodhall, N.; Jones, D. L. Comparative Assessment of Filtration- and Precipitation-Based Methods for the Concentration of SARS-CoV-2 and Other Viruses from Wastewater. *Microbiol. Spectr.* **2022**, *10* (4), e01102-22. https://doi.org/10.1128/spectrum.01102-22.

(16) Anderson-Coughlin, B. L.; Shearer, A. E. H.; Omar, A. N.; Wommack, K. E.; Kniel, K. E. Recovery of SARS-CoV-2 from Wastewater Using Centrifugal Ultrafiltration. *Methods Protoc.* **2021**, *4* (2), 32. https://doi.org/10.3390/mps4020032.

(17) Sapula, S. A.; Whittall, J. J.; Pandopulos, A. J.; Gerber, C.; Venter, H. An Optimized and Robust PEG Precipitation Method for Detection of SARS-CoV-2 in Wastewater. *Sci. Total Environ.* **2021**, *785*, 147270. https://doi.org/10.1016/j.scitotenv.2021.147270.

(18) Philo, S. E.; Ong, A. Q. W.; Keim, E. K.; Swanstrom, R.; Kossik, A. L.; Zhou, N. A.; Beck, N. K.; Meschke, J. S. Development and Validation of the Skimmed Milk Pellet Extraction Protocol for SARS-CoV-2 Wastewater Surveillance. *Food Environ. Virol.* **2022**, *14* (4), 355–363. https://doi.org/10.1007/s12560-022-09512-5.

(19) Fonseca, M. S.; Machado, B. A. S.; Rolo, C. de A.; Hodel, K. V. S.; Almeida, E. dos S.; de Andrade, J. B. Evaluation of SARS-CoV-2 Concentrations in Wastewater and River Water Samples. *Case Stud. Chem. Environ. Eng.* **2022**, *6*, 100214. https://doi.org/10.1016/j.cscee.2022.100214.

(20) Bhatnagar, B. S.; Tchessalov, S.; Lewis, L. M.; Johnson, R. Freeze Drying of Biologics. In *Encyclopedia of Pharmaceutical Science and Technology, Six Volume Set (Print)*; CRC Press, 2013.

(21) Alves, D.; Sparrow, R.; Garnier, G. Rapidly Freeze-Dried Human Red Blood Cells for Pre-Transfusion Alloantibody Testing Reagents. *J. Biomed. Mater. Res. B Appl. Biomater.* **2021**, *109* (11), 1689–1697. https://doi.org/10.1002/jbm.b.34825.

(22) Qin, C.; Chen, C.; Shang, C.; Xia, K. Fe3+-Saturated Montmorillonite Effectively Deactivates Bacteria in Wastewater. *Sci. Total Environ.* **2018**, *622–623*, 88–95. https://doi.org/10.1016/j.scitotenv.2017.11.302.

(23) Medema, G.; Heijnen, L.; Elsinga, G.; Italiaander, R.; Brouwer, A. Presence of SARS-Coronavirus-2 RNA in Sewage and Correlation with Reported COVID-19 Prevalence in the Early Stage of the Epidemic in The Netherlands. *Environ. Sci. Technol. Lett.* **2020**, *7* (7), 511–516. https://doi.org/10.1021/acs.estlett.0c00357.

(24) Fontenele, R. S.; Kraberger, S.; Hadfield, J.; Driver, E. M.; Bowes, D.; Holland, L. A.; Faleye, T. O. C.; Adhikari, S.; Kumar, R.; Inchausti, R.; Holmes, W. K.; Deitrick, S.; Brown, P.; Duty, D.; Smith, T.; Bhatnagar, A.; Yeager, R. A.; Holm, R. H.; von Reitzenstein, N. H.; Wheeler, E.; Dixon, K.; Constantine, T.; Wilson, M. A.; Lim, E. S.; Jiang, X.; Halden, R. U.; Scotch, M.; Varsani, A. High-Throughput Sequencing of SARS-CoV-2 in Wastewater Provides Insights into Circulating Variants. *Water Res.* **2021**, *205*, 117710. https://doi.org/10.1016/j.watres.2021.117710.

(25) Gonçalves, J.; Koritnik, T.; Mioč, V.; Trkov, M.; Bolješič, M.; Berginc, N.; Prosenc, K.; Kotar, T.; Paragi, M. Detection of SARS-CoV-2 RNA in Hospital Wastewater from a Low COVID-19 Disease Prevalence Area. *Sci. Total Environ.* **2021**, *755*, 143226. https://doi.org/10.1016/j.scitotenv.2020.143226.

(26) Kazenelson, J.; Jefferson, T.; Rhodes, R. G.; Cahoon, L. B.; Frampton, A. R. Detection of SARS-CoV-2 RNA in Wastewater from an Enclosed College Campus Serves as an Early Warning Surveillance System. *PLOS ONE* **2023**, *18* (7), e0288808. https://doi.org/10.1371/journal.pone.0288808.

(27) CDC. *Laboratory Biosafety Guidelines for working with SARS-CoV-2*. COVID-19. https://www.cdc.gov/covid/php/lab/index.html (accessed 2025-11-05).

(28) Patterson, E. I.; Prince, T.; Anderson, E. R.; Casas-Sanchez, A.; Smith, S. L.; Cansado-Utrilla, C.; Solomon, T.; Griffiths, M. J.; Acosta-Serrano, Á.; Turtle, L.; Hughes, G. L. Methods of Inactivation of SARS-CoV-2 for Downstream Biological Assays. *J. Infect. Dis.* **2020**, *222* (9), 1462–1467. https://doi.org/10.1093/infdis/jiaa507.

(29) Lu, X.; Wang, L.; Sakthivel, S. K.; Whitaker, B.; Murray, J.; Kamili, S.; Lynch, B.; Malapati, L.; Burke, S. A.; Harcourt, J.; Tamin, A.; Thornburg, N. J.; Villanueva, J. M.; Lindstrom, S. US CDC Real-Time Reverse Transcription PCR Panel for Detection of Severe Acute Respiratory Syndrome Coronavirus 2. *Emerg. Infect. Dis.* **2020**, *26* (8), 1654–1665. https://doi.org/10.3201/eid2608.201246.

(30) Lei, C.; Yang, J.; Hu, J.; Sun, X. On the Calculation of TCID50 for Quantitation of Virus Infectivity. *Virol. Sin.* **2020**, *36* (1), 141–144. https://doi.org/10.1007/s12250-020-00230-5.

(31) Dare, R. K.; Fry, A. M.; Chittaganpitch, M.; Sawanpanyalert, P.; Olsen, S. J.; Erdman, D. D. Human Coronavirus Infections in Rural Thailand: A Comprehensive Study Using Real-Time Reverse-Transcription Polymerase Chain Reaction Assays. *J. Infect. Dis.* **2007**, *196* (9), 1321–1328. https://doi.org/10.1086/521308.

(32) FRALICK, D.; ZHENG, J. Z.; Wang, B.; TU, X. M.; FENG, C. The Differences and Similarities Between Two-Sample T-Test and Paired T-Test. *Shanghai Arch. Psychiatry 29* (3), 184–188. https://doi.org/10.11919/j.issn.1002-0829.217070.

(33) Souza, R. R. de; Toebe, M.; Mello, A. C.; Bittencourt, K. C. Sample Size and Shapiro-Wilk Test: An Analysis for Soybean Grain Yield. *Eur. J. Agron.* **2023**, *142*, 126666. https://doi.org/10.1016/j.eja.2022.126666.

(34) Hauke, J.; Kossowski, T. Comparison of Values of Pearson's and Spearman's Correlation Coefficients on the Same Sets of Data. *Sciendo* **2011**. https://doi.org/10.2478/v10117-011-0021-1.
(35) Posit team. RStudio: Integrated Development Environment for R, 2025. http://www.posit.co/.
(36) Nagelkerke, E.; Hetebrij, W. A.; Koelewijn, J. M.; Kooij, J.; van der Drift, A.-M. R.; van der Beek, R. F. H. J.; de Jonge, E. F.; Lodder, W. J. PCR Standard Curve Quantification in an Extensive Wastewater Surveillance Program: Results from the Dutch SARS-CoV-2 Wastewater Surveillance. *Front. Public Health* **2023**, *11*, 1141494. https://doi.org/10.3389/fpubh.2023.1141494.
(37) Chomczynski, P.; Sacchi, N. The Single-Step Method of RNA Isolation by Acid Guanidinium Thiocyanate–Phenol–Chloroform Extraction: Twenty-Something Years On. *Nat. Protoc.* **2006**, *1* (2), 581–585. https://doi.org/10.1038/nprot.2006.83.
(38) Fabre, A.-L.; Colotte, M.; Luis, A.; Tuffet, S.; Bonnet, J. An Efficient Method for Long-Term Room Temperature Storage of RNA. *Eur. J. Hum. Genet.* **2014**, *22* (3), 379–385. https://doi.org/10.1038/ejhg.2013.145.
(39) Thatcher, S. A. DNA/RNA Preparation for Molecular Detection. *Clin. Chem.* **2015**, *61* (1), 89–99. https://doi.org/10.1373/clinchem.2014.221374.
(40) Ramachandran, K. M.; Tsokos, C. P. Chapter 12 - Nonparametric Tests. In *Mathematical Statistics with Applications in R (Second Edition)*; Ramachandran, K. M., Tsokos, C. P., Eds.; Academic Press: Boston, 2015; pp 589–637. https://doi.org/10.1016/B978-0-12-417113-8.00012-6.
(41) Hutchison, J. M.; Li, Z.; Chang, C.-N.; Hiripitiyage, Y.; Wittman, M.; Sturm, B. S. M. Improving Correlation of Wastewater SARS-CoV-2 Gene Copy Numbers with COVID-19 Public Health Cases Using Readily Available Biomarkers. *FEMS Microbes* **2022**, *3*, xtac010. https://doi.org/10.1093/femsmc/xtac010.
(42) Hsu, S.-Y.; Bayati, M.; Li, C.; Hsieh, H.-Y.; Belenchia, A.; Klutts, J.; Zemmer, S. A.; Reynolds, M.; Semkiw, E.; Johnson, H.-Y.; Foley, T.; Wieberg, C. G.; Wenzel, J.; Johnson, M. C.; Lin, C.-H. Biomarkers Selection for Population Normalization in SARS-CoV-2 Wastewater-Based Epidemiology. *Water Res.* **2022**, *223*, 118985. https://doi.org/10.1016/j.watres.2022.118985.
(43) King, A.; Eckersley, R. Inferential Statistics IV: Choosing a Hypothesis Test; 2019; pp 147–171. https://doi.org/10.1016/B978-0-08-102939-8.00016-5.
(44) van Kampen, J. J. A.; van de Vijver, D. A. M. C.; Fraaij, P. L. A.; Haagmans, B. L.; Lamers, M. M.; Okba, N.; van den Akker, J. P. C.; Endeman, H.; Gommers, D. A. M. P. J.; Cornelissen, J. J.; Hoek, R. A. S.; van der Eerden, M. M.; Hesselink, D. A.; Metselaar, H. J.; Verbon, A.; de Steenwinkel, J. E. M.; Aron, G. I.; van Gorp, E. C. M.; van Boheemen, S.; Voermans, J. C.; Boucher, C. A. B.; Molenkamp, R.; Koopmans, M. P. G.; Geurtsvankessel, C.; van der Eijk, A. A. Duration and Key Determinants of Infectious Virus Shedding in Hospitalized Patients with Coronavirus Disease-2019 (COVID-19). *Nat. Commun.* **2021**, *12* (1), 267. https://doi.org/10.1038/s41467-020-20568-4.
(45) Xing, Y.-H.; Ni, W.; Wu, Q.; Li, W.-J.; Li, G.-J.; Wang, W.-D.; Tong, J.-N.; Song, X.-F.; Wing-Kin Wong, G.; Xing, Q.-S. Prolonged Viral Shedding in Feces of Pediatric Patients with Coronavirus Disease 2019. *J. Microbiol. Immunol. Infect.* **2020**. https://doi.org/10.1016/j.jmii.2020.03.021.

(46) Randazzo, W.; Truchado, P.; Cuevas-Ferrando, E.; Simón, P.; Allende, A.; Sánchez, G. SARS-CoV-2 RNA in Wastewater Anticipated COVID-19 Occurrence in a Low Prevalence Area. *Water Res.* **2020**, *181*, 115942. https://doi.org/10.1016/j.watres.2020.115942.
(47) Kuang, D.; Gao, X.; Du, N.; Huang, J.; Dai, Y.; Chen, Z.; Wang, Y.; Wang, C.; Lu, R. Wastewater Surveillance as a Predictive Tool for COVID-19: A Case Study in Chengdu. https://doi.org/10.1371/journal.pone.0324521.
(48) Gonzalez, R.; Curtis, K.; Bivins, A.; Bibby, K.; Weir, M. H.; Yetka, K.; Thompson, H.; Keeling, D.; Mitchell, J.; Gonzalez, D. COVID-19 Surveillance in Southeastern Virginia Using Wastewater-Based Epidemiology. *Water Res.* **2020**, *186*, 116296. https://doi.org/10.1016/j.watres.2020.116296.
(49) Kitajima, M.; Ahmed, W.; Bibby, K.; Carducci, A.; Gerba, C. P.; Hamilton, K. A.; Haramoto, E.; Rose, J. B. SARS-CoV-2 in Wastewater: State of the Knowledge and Research Needs. *Sci. Total Environ.* **2020**, *739*, 139076. https://doi.org/10.1016/j.scitotenv.2020.139076.
(50) Ye, Y.; Ellenberg, R. M.; Graham, K. E.; Wigginton, K. R. Survivability, Partitioning, and Recovery of Enveloped Viruses in Untreated Municipal Wastewater. *Environ. Sci. Technol.* **2016**, *50* (10), 5077–5085. https://doi.org/10.1021/acs.est.6b00876.
(51) Ahmed, W.; Bertsch, P. M.; Bibby, K.; Haramoto, E.; Hewitt, J.; Huygens, F.; Gyawali, P.; Korajkic, A.; Riddell, S.; Sherchan, S. P.; Simpson, S. L.; Sirikanchana, K.; Symonds, E. M.; Verhagen, R.; Vasan, S. S.; Kitajima, M.; Bivins, A. Decay of SARS-CoV-2 and Surrogate Murine Hepatitis Virus RNA in Untreated Wastewater to Inform Application in Wastewater-Based Epidemiology. *Environ. Res.* **2020**, *191*, 110092. https://doi.org/10.1016/j.envres.2020.110092.

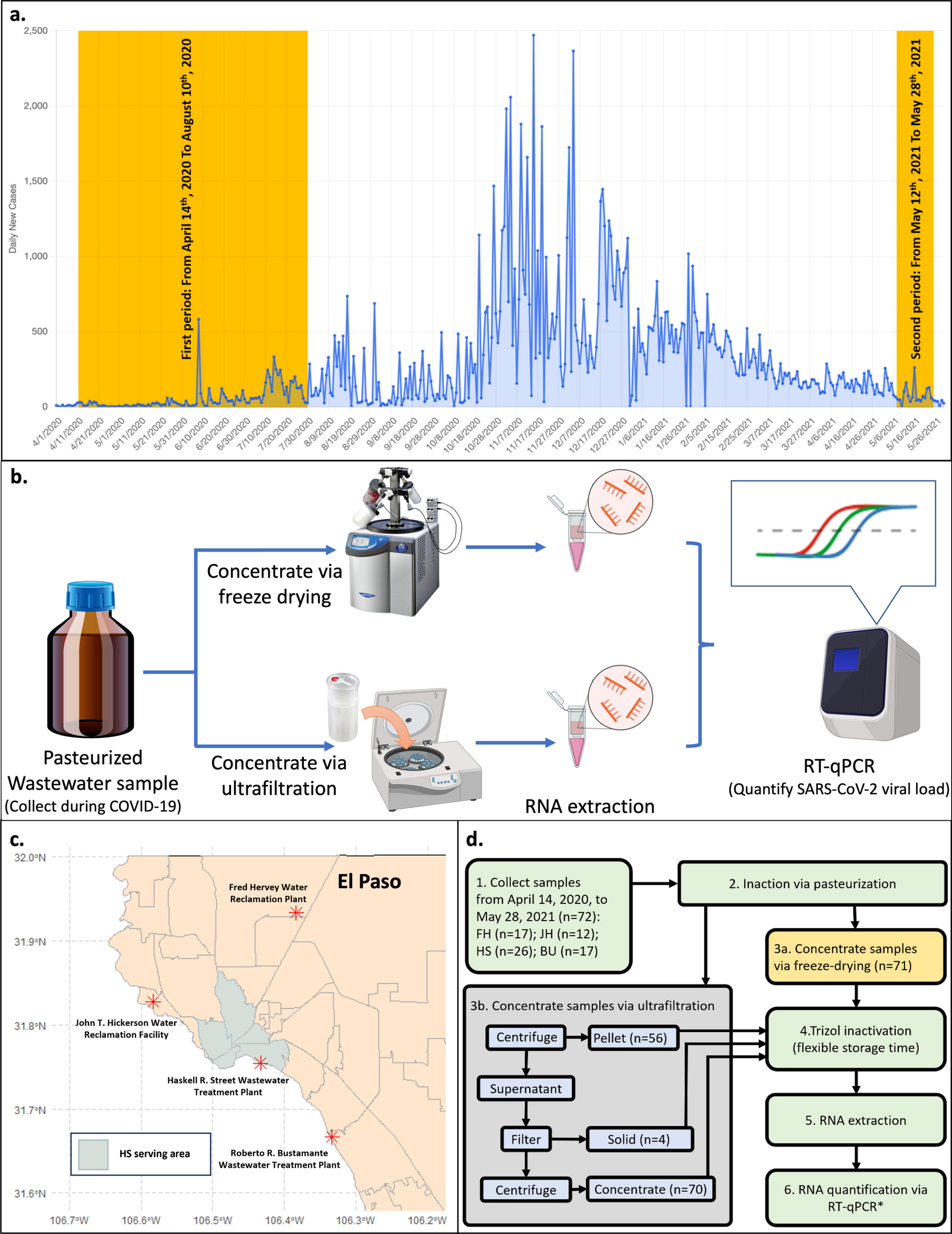
a.
Daily New Cases
2,500
2,000
1,500
1,000
500
0
First period: From April 14th, 2020 To August 10th, 2020
Second period: From May 12th, 2021 To May 28th, 2021
4/1/2020
4/11/2020
4/21/2020
5/1/2020
5/11/2020
5/21/2020
5/31/2020
6/10/2020
6/20/2020
6/30/2020
7/10/2020
7/20/2020
7/30/2020
8/9/2020
8/19/2020
8/29/2020
9/8/2020
9/18/2020
9/28/2020
10/8/2020
10/18/2020
10/28/2020
11/7/2020
11/17/2020
11/27/2020
12/7/2020
12/17/2020
12/27/2020
1/6/2021
1/16/2021
1/26/2021
2/5/2021
2/15/2021
2/25/2021
3/7/2021
3/17/2021
3/27/2021
4/6/2021
4/16/2021
4/26/2021
5/6/2021
5/16/2021
5/26/2021
b.
Pasteurized Wastewater sample
(Collect during COVID-19)
Concentrate via freeze drying
Concentrate via ultrafiltration
RNA extraction
RT-qPCR
(Quantify SARS-CoV-2 viral load)
c.
El Paso
Fred Hervey Water Reclamation Plant
John T. Hickerson Water Reclamation Facility
Haskell R. Street Wastewater Treatment Plant
Roberto R. Bustamante Wastewater Treatment Plant
HS serving area
32.0°N
31.9°N
31.8°N
31.7°N
31.6°N
106.7°W
106.6°W
106.5°W
106.4°W
106.3°W
106.2°W
d.
1. Collect samples from April 14, 2020, to May 28, 2021 (n=72): FH (n=17); JH (n=12); HS (n=26); BU (n=17)
2. Inaction via pasteurization
3a. Concentrate samples via freeze-drying (n=71)
3b. Concentrate samples via ultrafiltration
Centrifuge
Pellet (n=56)
Supernatant
Filter
Solid (n=4)
Centrifuge
Concentrate (n=70)
4.Trizol inactivation (flexible storage time)
5. RNA extraction
6. RNA quantification via RT-qPCR*

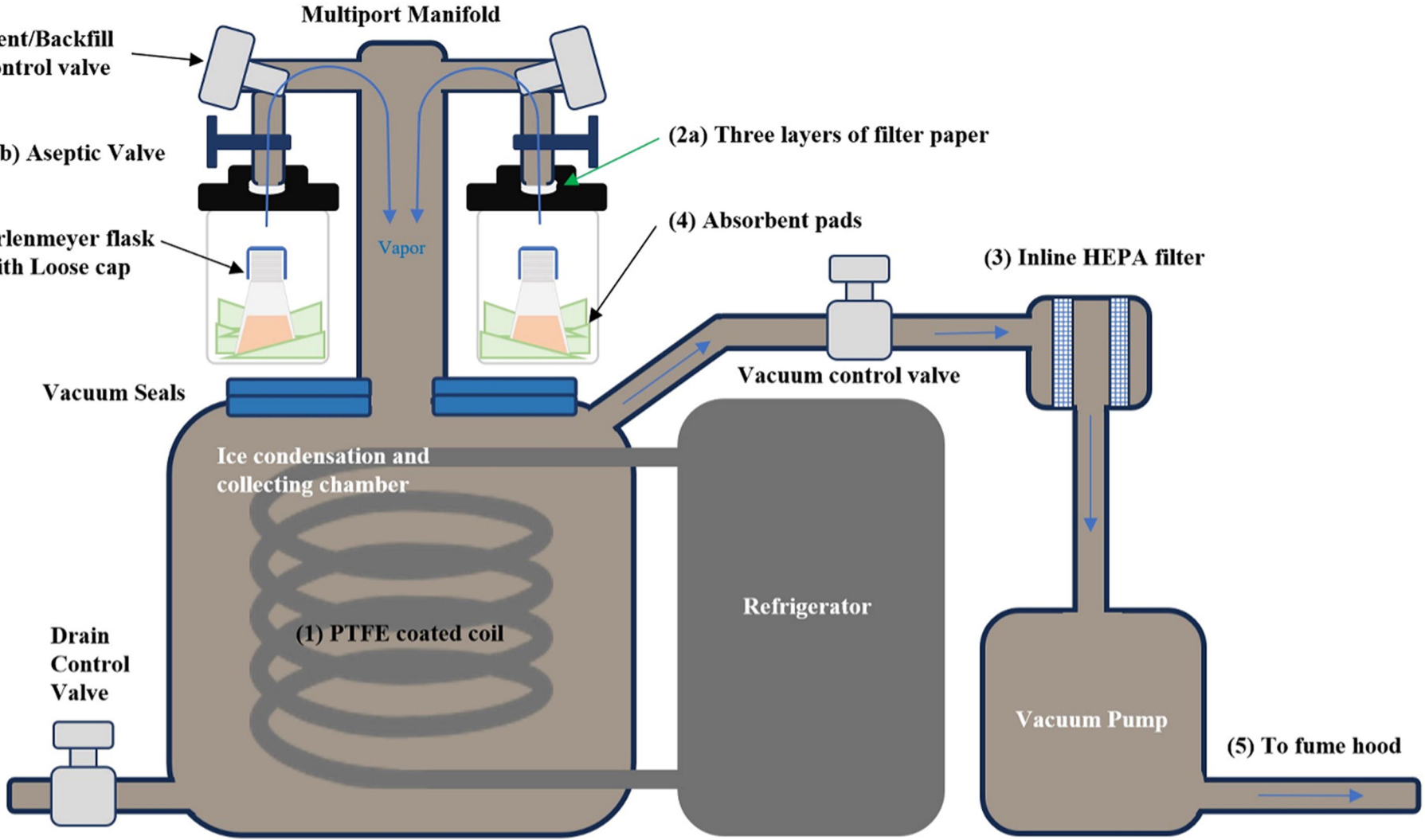
Multiport Manifold
Vent/Backfill control valve
(2b) Aseptic Valve
(2a) Three layers of filter paper
Erlenmeyer flask with Loose cap
Vapor
(4) Absorbent pads
(3) Inline HEPA filter
Vacuum control valve
Vacuum Seals
Ice condensation and collecting chamber
Refrigerator
(1) PTFE coated coil
Drain Control Valve
Vacuum Pump
(5) To fume hood

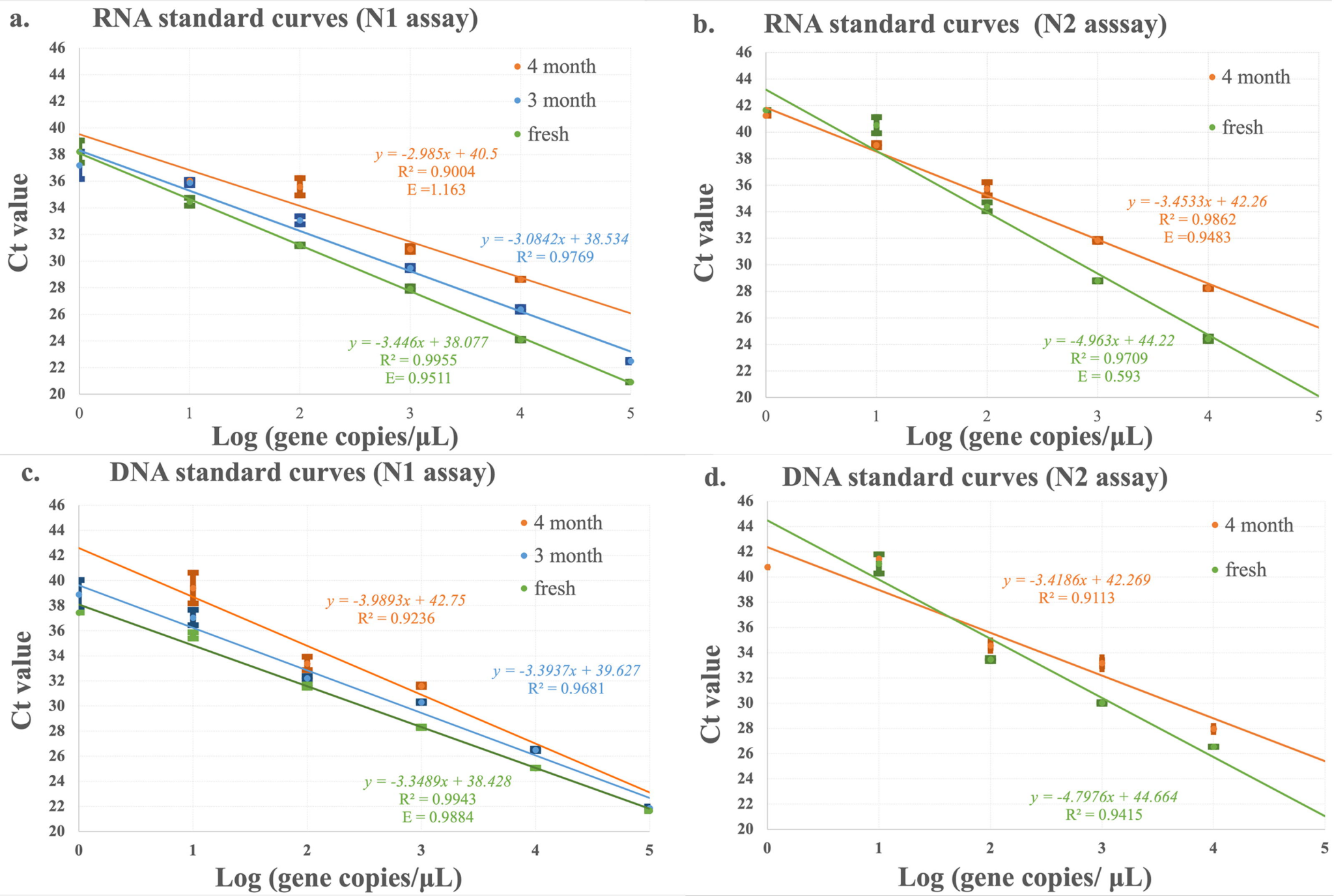
a.
RNA standard curves (N1 assay)
4 month
3 month
fresh
y = -2.985x + 40.5
R² = 0.9004
E =1.163
y = -3.0842x + 38.534
R² = 0.9769
y = -3.446x + 38.077
R² = 0.9955
E= 0.9511
Ct value
Log (gene copies/µL)
b.
RNA standard curves (N2 asssay)
4 month
fresh
y = -3.4533x + 42.26
R² = 0.9862
E =0.9483
y = -4.963x + 44.22
R² = 0.9709
E = 0.593
Ct value
Log (gene copies/µL)
c.
DNA standard curves (N1 assay)
4 month
3 month
fresh
y = -3.9893x + 42.75
R² = 0.9236
y = -3.3937x + 39.627
R² = 0.9681
y = -3.3489x + 38.428
R² = 0.9943
E = 0.9884
Ct value
Log (gene copies/µL)
d.
DNA standard curves (N2 assay)
4 month
fresh
y = -3.4186x + 42.269
R² = 0.9113
y = -4.7976x + 44.664
R² = 0.9415
Ct value
Log (gene copies/ µL)